

Fiber based frequency-degenerate polarization entangled photon pair sources for information encoding

FENG ZHU, WEI ZHANG,* AND YIDONG HUANG

Tsinghua National Laboratory for Information Science and Technology, Department of Electronic Engineering, Tsinghua University, Beijing 100084, China

*zwei@tsinghua.edu.cn

Abstract: In this paper, a generation scheme of telecom band frequency-degenerate polarization entangled photon pairs is proposed and demonstrated experimentally. It is based on the vector spontaneous four wave mixing (SFWM) process in a Sagnac fiber loop, in which two frequency-degenerate and polarization orthogonal biphoton states have equal probabilities for generating along the clockwise and counter-clockwise directions. The quantum interference between them at the 50:50 fiber coupler of the fiber loop separates the two frequency-degenerate photons in a pair, leading to the generation of polarization entanglement. The raw fringe visibilities of the two-photon interferences under two non-orthogonal polarization bases are 91% and 90%, respectively. Information can be encoded on the generated photon pairs using the polarization entangled Bell states, which requires the frequency-degenerate property. It is demonstrated by a simplified Bell state measurement with a fringe visibility of 83%.

© 2016 Optical Society of America

OCIS codes: (270.0270) Quantum optics; (190.4370) Nonlinear optics, fibers; (270.5585) Quantum information and processing.

References and links

1. A. Einstein, B. Podolsky, and N. Rosen, "Can quantum-mechanical description of physical reality be considered complete?" *Phys. Rev.* **47**, 777 (1935).
2. A. Aspect, P. Grangier, and G. Roger, "Experimental realization Of Einstein-Podolsky-Rosen-Bohm Gedankenexperiment a new violation Of Bell inequalities," *Phys. Rev. Lett.* **49**(2) 91–94 (1982).
3. A. K. Ekert, "Quantum cryptography based on Bell Theorem," *Phys. Rev. Lett.* **67**, 661–663 (1991).
4. Y. I. Bogdanov, M. V. Chekhova, S. P. Kulik, G. A. Maslennikov, A. A. Zhukov, C. H. Oh, and M. K. Tey, "Qutrit state engineering with biphotons," *Phys. Rev. Lett.* **93**, 230503 (2004).
5. H. Weinfurter, "New High-Intensity Source of Polarization-Entangled Photon Pairs," *Europhys. Lett.* **25**, 559 (1994).
6. D. F. V. James, P. G. Kwiat, W. J. Munro, and A. G. White, "Measurement of qubits," *Phys. Rev. A* **64**, 052312 (2001).
7. D. Bouwmeester, J. W. Pan, K. Mattle, M. Eibl, H. Weinfurter, A. Zeilinger, "Experimental quantum teleportation," *Nature (London)* **390**, 575 (1997).
8. J. W. Pan, D. Bouwmeester, H. Weinfurter, A. Zeilinger, "Experimental entanglement swapping: Entangling photons that never interacted," *Phys. Rev. Lett.* **80**, 31891 (2012).
9. H.-K. Lo, M. Curty, and B. Qi, "Measurement-device-independent quantum key distribution," *Phys. Rev. Lett.* **108**(13), 130503 (2012).
10. Y. Fu, H. L. Yin, T. Y. Chen, and Z. B. Chen, "Long-distance measurement-device-independent multiparty quantum communication," *Phys. Rev. Lett.* **114**, 090501 (2015).
11. J. W. Pan, Z. B. Chen, C. Y. Lu, H. Weinfurter, A. Zeilinger, and M. Zukowski, "Multiphoton entanglement and interferometry," *Rev. Mod. Phys.* **84**, 777 (2012).
12. K. Mattle, H. Weinfurter, P. G. Kwiat, and A. Zeilinger, "Dense coding in experimental quantum communication," *Phys. Rev. Lett.* **76**, 4656 (1996).
13. P. G. Kwiat, K. Mattle, H. Weinfurter, A. Zeilinger, A. V. Sergienko, and Y. Shih, "New high-intensity source of polarization-entangled photon pairs," *Phys. Rev. Lett.* **75**, 4337 (1995).
14. G. P. Agrawal, *Nonlinear Fiber Optics*, 3rd ed. (Academic, 2001).
15. X. Li, P. L. Voss, J. E. Sharping, and P. Kumar, "Optical-fiber source of polarization-entangled photons in the 1550 nm telecom band," *Phys. Rev. Lett.* **94**, 053601 (2005).
16. H. Takesue, and K. Inoue, "Generation of polarization-entangled photon pairs and violation of Bell's inequality using spontaneous four-wave mixing in a fiber loop," *Phys. Rev. A* **70**, 031802 (2004).

17. Q. Zhou, W. Zhang, J. Cheng, Y. Huang, and J. Peng, "Polarization-entangled bell states generation based on birefringence in high nonlinear microstructure fiber at 1.5 μm ," *Opt. Lett.* **34**(18), 2706–2708 (2009).
18. O. Cohen, J. Lundeen, B. Smith, G. Puentes, P. Mosley, and I. A. Walmsley, "Tailored photon-pair generation in optical fibers," *Phys. Rev. Lett.* **102**, 123603 (2009).
19. Q. Zhou, W. Zhang, P. Wang, Y. Huang, and J. Peng, "Polarization entanglement generation at 1.5 μm based on walk-off effect due to fiber birefringence," *Opt. Lett.* **37**(10), 1679–1681 (2012).
20. C. K. Hong, Z. Y. Ou, and L. Mandel, "Measurement of subpicosecond time intervals between two photons by interference," *Phys. Rev. Lett.* **59**, 2044 (1987).
21. M. Medic, J. B. Altepeter, M. A. Hall, M. Patel, and P. Kumar, "Fiber-based telecommunication-band source of degenerate entangled photons," *Opt. Lett.* **35**, 802–804 (2010).
22. E. Brainin, "Four-photon scattering in birefringent fibers," *Phys. Rev. A* **79**, 023840 (2009).
23. S. Dong, L. J. Yu, W. Zhang, J. J. Wu, W. J. Zhang, L. X. You, and Y. D. Huang, "Generation of hyper-entanglement in polarization/energy-time and discrete-frequency/energy-time in optical fibers," *Sci. Rep.* **5**, 9195 (2015).
24. J. K. He, B. A. Bell, A. Casas-Bedoya, Y. B. Zhang, A. S. Clark, C. L. Xiong, and B. J. Eggleton, "Ultracompact quantum splitter of degenerate photon pairs," *Optica* **2**, 779–782 (2015).
25. W. P. Grice, "Arbitrarily complete Bell-state measurement using only linear optical elements," *Phys. Rev. A* **84**, 042331 (2011).
26. J. Fulconis, O. Alibart, W. J. Wadsworth, and J. G. Rarity, "Quantum interference with photon pairs using two micro-structured fibres," *New J. Phys.* **9**, 276 (2007).

1. Introduction

Entanglement is an important resource in quantum communication and quantum information processing [1–3]. Information can be encoded on entangled states, then decoded to realize specific quantum functions after quantum state processing and transmission [4–6]. The polarization entangled biphoton Bell states are the most popular in the research using quantum coding to realize this kind of information encoding [7–10]. They are four orthogonal biphoton states with maximum polarization entanglement. Any one of them can be transformed to the other three by a specific polarization manipulation on one photon of a pair [11]. And they can be discriminated by the polarization Bell state measurement (BSM) [5], which provide the way to decode the information. Hence, they have been widely used in many quantum information applications, such as quantum teleportation [7] and quantum dense coding [12].

The most popular schemes to generate polarization entangled Bell states are based on spontaneous down conversion (SPDC) in nonlinear crystals [13]. Usually they operated in 800nm band. In recent years, as the development of quantum information applications over optical fibers, telecom band quantum light sources based on the spontaneous four wave mixing (SFWM) in optical fibers have attracted much attention [14]. Based on this mechanism, several schemes for telecom band polarization entanglement generation have been proposed. Most of them utilize the degenerate-pump SFWM process, in which the generated signal and idler photons are selected in different frequencies [15–19]. Hence, although the generated photon pairs are polarization entangled, they can not be used in information encoding based on the Bell states, which can be discriminated by the BSM [20]. In 2010, Medic *et al* proposed and demonstrate a scheme of frequency-degenerate polarization entangled photon pair generation based on fiber [21]. In their scheme, pulsed pump lights with two different wavelengths are applied on two orthogonal polarization axes of a Sagnac fiber loop. A polarization dependent delay (PDD) unit is used to provide a time difference between the pulsed pump lights along the two axes, by which frequency-degenerate biphoton states polarized along the two axes are generated independently by the scalar SFWM processes. In each axis, the two photons in a pair output from the two ports of the fiber loop. Then another two PDD units are used to realize the temporal and spatial superposition of the generated photons along the two axes, leading to the polarization entangled state generation. An experiment of Hong-Ou-Mandel (HOM) interference between the two photons in a pair generated along a specific axis was taken to show its potential on realizing the polarization entangled Bell states, which can be discriminated by the BSM.

In this paper, we proposed a different scheme for telecom band frequency-degenerate polarization entangled photon pair generation based on optical fiber. It based on the quantum interference of the biphoton states generated by the vector SFWM processes in a Sagnac fiber loop. Comparing with the scheme in Ref. [21], the PDD units are no longer required since the temporal and spatial superposition of the generated biphoton states is ensured in the interference process intrinsically. The polarization entanglement of the generated state is demonstrated by the two-photon interferences under two non-orthogonal polarization bases. Its potential on realizing the polarization entangled Bell pairs for information encoding is demonstrated by a simplified BSM experiment directly.

2. Principle

The SFWM provides an effective way to generate photon-pairs in $\chi^{(3)}$ nonlinear media, especially in silica optical fibers. In the SFWM, two pump photons are annihilated, and a pair of photons, named as ‘signal’ and ‘idler’ respectively, are generated simultaneously. Their frequencies can be denoted by ω_{p1} , ω_{p2} , ω_s and ω_i respectively, which satisfy the relation of $\omega_{p1} + \omega_{p2} = \omega_s + \omega_i$ due to the energy conservation in this process. If the process is initiated by two pump lights with different frequencies and a proper filter is used to select the signal and idler photons with the same frequency, the generation of frequency-degenerate photon pairs can be realized, with the relation that $\omega_s = \omega_i = (\omega_{p1} + \omega_{p2})/2$.

According to the polarization relation between the annihilated pump photons and generated signal and idler photons, there are several types of SFWM processes [14, 15, 18, 22]. The most popular one is the scalar SFWM process [15], in which all the photons are polarized along the same direction. In this work, we utilize a specific type of vector SFWM processes which is shown in Fig. 1(a).

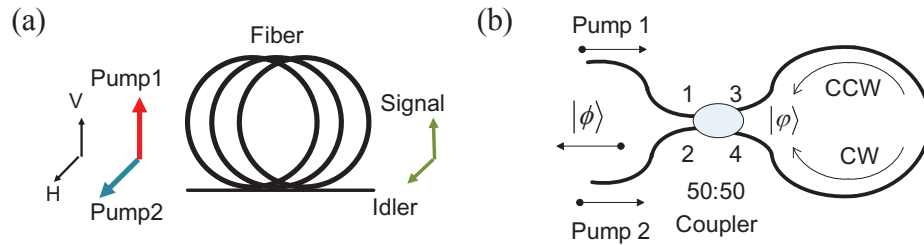


Fig. 1. (a) Sketch of the vector SFWM used in this scheme. (b) Diagram of the quantum interference in the Sagnac fiber loop.

In this process, the two annihilated pump photons are polarized in two orthogonal polarization axes and so are the generated signal and idler photons. Theoretical analysis has shown that the efficiency of this vector SFWM process is 4/9 of that of the scalar SFWM process, if the two polarization components of the pump light are equal and their phase matching conditions are satisfied [22]. Usually, the two orthogonal polarization axes in the fiber are indicated as the vertical and horizontal axes, which can be denoted by H and V, respectively. When the two pumps with frequencies of ω_{p1} and ω_{p2} are injected into the optical fiber with the polarization directions of H and V, respectively, the generated biphoton state by this vector process can be expressed as $|\phi\rangle = [1 + \gamma \hat{a}_H^\dagger \hat{a}_V^\dagger + O(\gamma^2)]|vac\rangle$, where γ is the amplitude of the vector SFWM process, \hat{a}_H^\dagger and \hat{a}_V^\dagger are the creation operators in the polarization axes of H and V, respectively. Since the two generated photons are frequency-degenerate, they are denoted by their polarizations (H and V).

To generate the polarization entangled photon pairs, we connect the optical fiber with a 50:50

fiber coupler to realize a Sagnac fiber loop, which is shown in Fig. 1(b). The two pumps (denoted by Pump 1 and Pump 2, respectively) are injected into the Sagnac fiber loop from Port 1 and 2, respectively, with orthogonal polarization directions. Both of them split to two components with the same power along CW and CCW directions. The coupler gives a $\frac{\pi}{2}$ phase shift between the two directions for each pump [24]. The pumps initiate the vector SFWM processes in the optical fiber bidirectionally, and there is equal probability for generating frequency-degenerate biphoton states along the clockwise (CW) and counter-clockwise (CCW) directions. Since the two pump lights are injected into the fiber loop in different ports, the additional phases on the two biphoton states along the CW and CCW directions are the same due to the symmetry of the Sagnac fiber loop [24]. Hence, the state at two port inside the fiber loop (3 and 4) can be written as

$$|\varphi\rangle = [1 + \gamma(\hat{a}_{3,H}^\dagger \hat{a}_{3,V}^\dagger + \hat{a}_{4,H}^\dagger \hat{a}_{4,V}^\dagger) + O(\gamma^2)]|vac\rangle \quad (1)$$

After the interference in the 50:50 fiber coupler, the biphoton states output from the two ports of the fiber loop (1 and 2) can be expressed as

$$\begin{aligned} |\phi\rangle &= [1 + \gamma(\frac{\hat{a}_{1,H}^\dagger + i\hat{a}_{2,H}^\dagger}{\sqrt{2}} \frac{\hat{a}_{1,V}^\dagger + i\hat{a}_{2,V}^\dagger}{\sqrt{2}} + \frac{\hat{a}_{2,H}^\dagger + i\hat{a}_{1,H}^\dagger}{\sqrt{2}} \frac{\hat{a}_{2,V}^\dagger + i\hat{a}_{1,V}^\dagger}{\sqrt{2}}) + O(\gamma^2)]|vac\rangle \\ &= [1 + i\gamma(\hat{a}_{1,H}^\dagger \hat{a}_{2,V}^\dagger + \hat{a}_{1,V}^\dagger \hat{a}_{2,H}^\dagger) + O(\gamma^2)]|vac\rangle \end{aligned} \quad (2)$$

where $\hat{a}_{i,X}^\dagger$ is the creation operator for the photon at the port of i with the polarization of X ($i \in \{1, 2, 3, 4\}$ and $X \in \{H, V\}$, respectively). It can be seen that the two frequency-degenerate photons in this state output from different ports, with the maximum polarization entanglement. It is worth noting that in Ref. [24], since the scalar SFWM process is used, the two frequency-degenerate photons output from the two ports are in the same polarization. Hence, it is only realize a function of "quantum separator". In the scheme proposed in this paper, the two output photons are in orthogonal polarizations and have the property of polarization entanglement since the vector SFWM processes are utilized.

Since the generated photon pairs are frequency-degenerate, by proper polarization manipulations on the two photons, different polarization entangled Bell states can be realized, which can be distinguished by the BSM. Hence, it can be used in information encoding.

3. The experiment

3.1. The experiment setup and its property of photon pair generation

The experiment setup is shown in Fig. 2, in which the inset figure shows the setup of the pump light source. To generate frequency-degenerate signal/idler photons with orthogonal polarizations, two pulsed pump lights with different frequencies and orthogonal polarizations are required. In the source, the output of a mode-locked erbium doped fiber laser with a repetition rate of 40 MHz is directed into a filtering system made of two commercial dense wavelength division multiplexers (DWDMs), by which two pulsed pump lights at 1552.52 nm and 1546.12 nm are filtered out. They are amplified by an erbium doped fiber amplifier (EDFA) and their powers are controlled by a variable optical attenuator (VOA). A 5/95 coupler is used to monitor the pump power. The light are separated by another filter system made of cascaded DWDMs, which narrows the linewidth of each pump light to 60 GHz and provides a side-band suppression of 120 dB to reject the noise photons at the wavelengths of signal photons and idler photons (1549.32 nm). The pulse width of the two pump lights are about 20 ps.

The main part of the experiment setup shown in Fig. 2 is a Sagnac fiber loop composed of a 50:50 fiber coupler (The splitting ratio is 50.5/49.5 for the component in the setup), a piece of dispersion shifted fiber (DSF) and a fiber polarization controller. The DSF is used as the nonlinear medium for the biphoton state generation, which is 250 meter in length. The DSF is

cooled to 2 K by a cryostat to suppress Spontaneous Raman scattering (SpRS). The polarization controller is used to maximum the quantum interference in the Sagnac fiber loop. The pump lights inject into the two ports of the 50:50 fiber coupler through two filters. An optical delay-line (ODL) is used to make sure that their pulses arrive the 50:50 fiber coupler at the same time. A variable optical attenuator (VOA) is used to make sure that the powers of the pump lights in the fiber loop are the same. Two fiber polarization controllers (PCs) are used to adjust the polarization of the two pump lights respectively and make them orthogonal in the Sagnac fiber loop. Initiated by the two pump lights, polarization orthogonal biphoton states are generated by the vector SFWM along the CW and CCW directions in the fiber loop, respectively, and interfere at the 50:50 fiber coupler. According to Section 2, this pumping scheme leads to a splitting biphoton state with polarization entanglement. Two optical filters made by cascaded DWDMs are used to select photons with degenerate frequency in the two paths (Path 1 and Path 2), realizing the generation of the frequency-degenerate polarization entangled state.

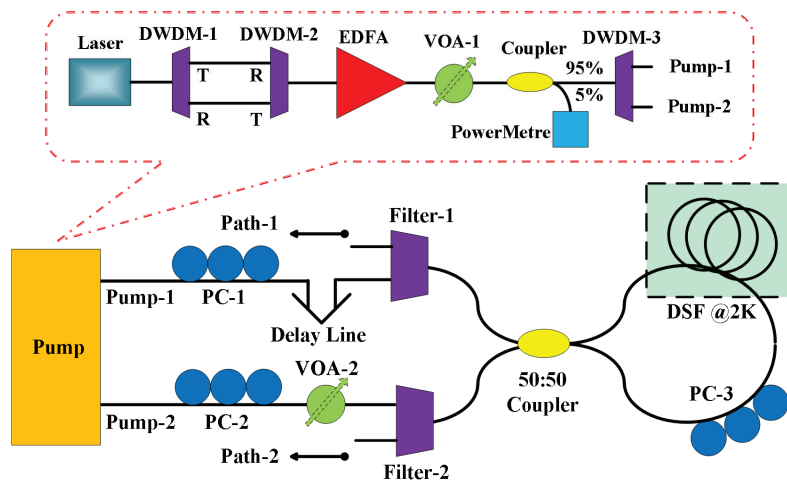


Fig. 2. Sketch of the experiment setup. DWDM: dense wavelength division multiplexer. T: Transmission port. R: Reflection port. EDFA: erbium doped fiber amplifier. VOA: variable optical attenuator. PC: polarization controller. DSF: dispersion shifted fiber.

Firstly, the generated photons are sent to two single photon detectors (SPDs) directly to show the property of photon pair generation in this setup. The two SPDs are based on InGaAs/InP avalanche photodiodes (ID220, IDQ Inc., Swiss), operating in the free running mode. Their efficiencies and dead times are set as 10% and 10 μ s, respectively. Their dark count rates are about 1 kHz. The detection events of the SPDs are recorded by a time correlated single photon counting module (TCSPC, DPC-230, Becker & Hickl GmbH Inc., Germany). The width of each time bin is 165 ps. The coincidence counts are the contributions in 8 bins covering the coincidence peak.

The experiment results are shown in Fig. 3. Fig. 3(a) is the results of the average single side counts under different pump levels, indicating by the total average pump power. The experimental data are fit by a quadratic polynomial, which is shown by the red curve. The black, blue and green lines indicate the contributions of the second-order, first-order and the constant terms. The second order term shows the contribution of photon generation by the SFWM, while other terms shows the impacts of noises, such as spontaneous Raman scattering, the leaky pump photons and the dark counts of detectors. It can be seen that the contribution of the generated photon pairs dominates under most pump level, showing that the noises are highly reduced in this setup by cooling the fiber to 2 K. The good performance of the photon pair generation

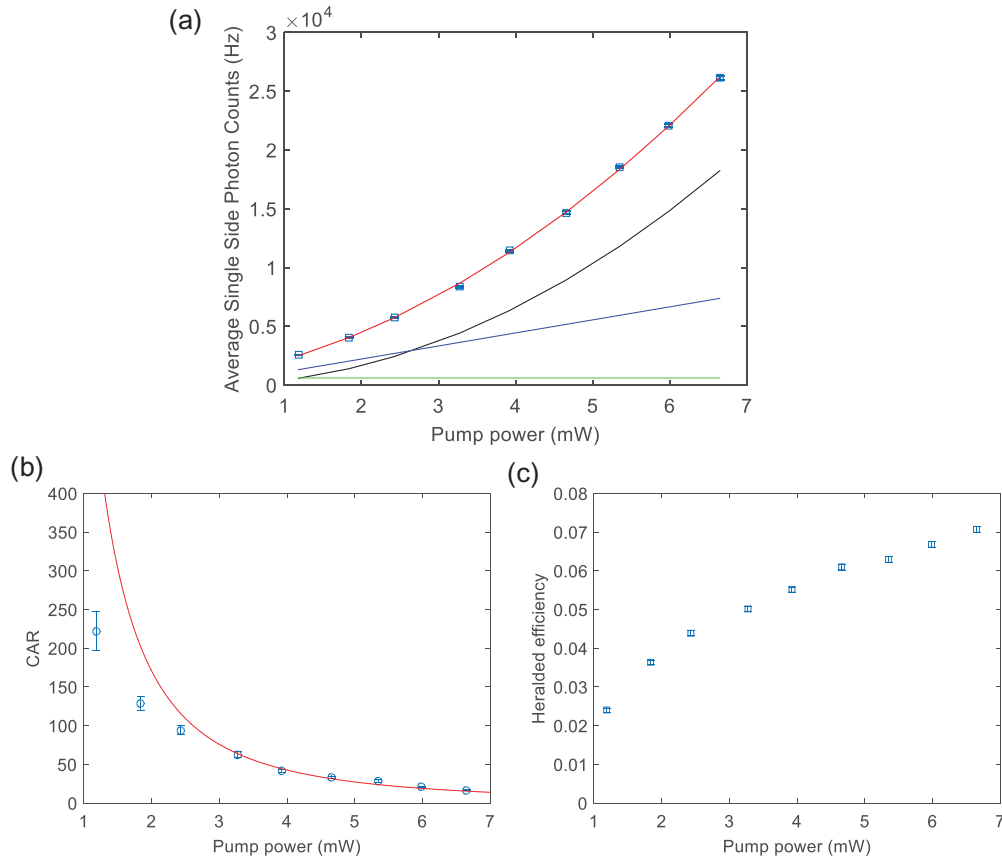


Fig. 3. The property of the photon pair generation in the setup. (a) The relation between the average single side photon counts and the pump power. The average single side photon counts are fit by a quadratic polynomial. The black, blue and green lines indicate the contributions of the second-order, first-order and the constant terms which show the contribution of photon generation by the SFWM, the spontaneous Raman scattering, the leaky pump photons and the dark counts of detectors. (b) The relation between the coincident to accidental coincidence ratio. The red line is the fitting curve of the six points under high pump levels. It is fitted by $CAR = \frac{A}{P^2}$, where P is the pump power. (c) The relation between the heralding efficiency and the pump power.

is also demonstrated by the measurement of the coincidence to accidental coincidence ratio (CAR) under different pump level, which is shown in Fig. 3(b). The experiment results under lower pump level are measured in larger time durations to reduce the error bars. The error bars come from the statistical error of the Poisson distribution of the photon counts. It can be seen that the CAR rises when the total average pump power decreases from 7 mW to 1 mW. Since the generation rate of photon pairs is in proportion to the square of the pump power and the CAR is inversely proportional to the photon pair generation rate if noise count is neglected [17], we fit the six points at right side with high pump levers by $CAR = \frac{A}{P^2}$, where P is the pump power. The fitting curve is shown as the red line in the figure. It can be seen that at high pump level, the measured CAR agrees with the curve very well. When the pump level reduces, the measured CAR is off the line due to the impact of noise count. The maximum CAR is larger than 200. In the following experiments, we set the total average pump power as 4 mW, hence,

a CAR of 50 can be expected. The heralding efficiency of the photon pair source is shown in Fig. 3(c), which is calculated by $N_{co}/(\eta N_s)$, where N_{co} , N_s and η are the coincidence counts, signal side photon counts and idler side efficiency of the SPD, respectively. It is mainly limited by the losses in the optical paths.

3.2. The experimental demonstration of the polarization entanglement

The property of polarization entanglement is demonstrated by the experiment of two photon interferences under two nonorthogonal polarization bases. In this experiment, the photons in the two output paths pass through half wave plates (HWPs) on rotation mounts and fixed polarizers, respectively. The polarization detecting angles of the two paths are decided by the twice of the angles of the corresponding HWPs. Then the photons in the two paths are detected by SPDs. Their coincidence counts are recorded in 90 seconds for each measurement. Fig. 4 shows the experiment results. The blue squares and red circles are the coincidence counts when the polarization detecting direction of one path varies and that of the other path is set as 0° and 45° , respectively. The blue and red lines are their fitting curves by the sinusoidal function. It can be seen that the raw visibility of the two curves are 91% and 90% respectively, larger than 70.7% (the non-classical threshold for the visibility of this two photon interference experiment [15]). This result is at the same level with typical works about the fiber based polarization entangled photon pair generation [15–19], showing that the generated photon pairs have good property of polarization entanglement. The visibility is mainly limited by the noise photons and dark counts, which is indicated by the CAR. The limited stability of the polarizations of the pump light and generated photon pairs also impacts the measurements, especially for the fringe in the diagonal basis.

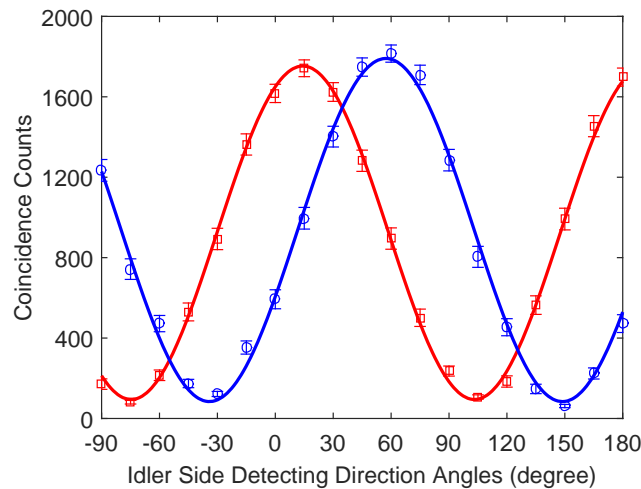


Fig. 4. The experimental results of two photon interferences under two nonorthogonal polarization bases. The blue squares and red circles are the coincidence counts when the polarization detecting direction of one path varies and that of the other path is set as 0° and 45° , respectively. The blue and red lines are their fitting curves by the sinusoidal function. The raw visibility of the two curves are 91% and 90% respectively.

3.3. BSM on the generated polarization-entangled Bell states

Since the generated photon pairs are frequency-degenerate, it can be used to prepare four polarization entangled Bell states, which can be discriminated by the Bell state measurement

(BSM) [5]. It provide a way to carry the information on the polarization entangled photon pairs. The widely used BSM scheme is based on linear optics. Based on a 50:50 beam splitter and two polarization beam splitters, this scheme can detect $\{|\psi^{(+)}\rangle\}$, $\{|\psi^{(-)}\rangle\}$, and $\{|\phi^{(+)}\rangle, |\phi^{(-)}\rangle\}$, however, $\{|\phi^{(+)}\rangle, |\phi^{(-)}\rangle\}$ can not be distinguished by this linear optical scheme. To distinguish all the four Bell states, the BSM scheme should be improved, for example, by introducing ancillary photons [25].

In this work, a simplified linear BSM [7] is used to demonstrate that the prepared polarization entangled photon pairs can be used to carry information. Using a 50:50 beam splitter, it is only able to distinguish $\{|\psi^{(-)}\rangle\}$ from the other three Bell states. The experiment setup is shown in Fig. 5(a). The two output paths of the photon pair sources are connected to a 50:50 fiber coupler, which is used as the 50:50 beam splitter in the simplified BSM. A fiber polarization controller is set on one path to copolarize the two paths. An optical delay line (ODL) is set on the other path to make the two photons in a pair pass through the 50:50 fiber coupler at the same time. A HWP is used to adjust the state of the photon pairs. The two output ports of the 50:50 fiber coupler are connected to the two SPDs and the coincidence counts are recorded.

The original state of the photon pairs generated by the proposed scheme is shown in Eq. (2). If the direction of the HWP is set to the direction of 'V', the state after the HWP become an anti-symmetric polarization Bell state

$$|\psi\rangle = (\hat{a}_{1,H}^\dagger \hat{a}_{2,V}^\dagger - \hat{a}_{1,V}^\dagger \hat{a}_{2,H}^\dagger)|vac\rangle/\sqrt{2} \quad (3)$$

This state can be discriminated by this simplified polarization BSM setup. While, the other three polarization Bell state can not be discriminated, i.e., there is no coincidence count if these states are detected by this setup. In the experiment, a symmetric state is used for comparison

$$|\psi'\rangle = (\hat{a}_{1,H}^\dagger \hat{a}_{2,H}^\dagger + \hat{a}_{1,V}^\dagger \hat{a}_{2,V}^\dagger)|vac\rangle/\sqrt{2} \quad (4)$$

which is realized by setting the HWP at an angle of 45° to the direction of "V".

The experiment results are shown in Fig. 5(b). The hollow squares and circles are the coincidence counts under different delay times of the ODL when the generated photon pairs are in the states in Eq. (3) and Eq. (4), respectively. The time for each event is 180 s. The red and green lines are their fitting curves by the Gaussian function. It can be seen that, for the state of Eq. (3), there is a coincidence peak when the delay of the ODL is 7.35 cm. This delay indicates the condition that the two photons in a pair pass through the 50:50 fiber coupler at the same time. Since the two photons are frequency-degenerate, the quantum interference in the 50:50 fiber coupler due to the indistinguishability of the two photon leads to the coincidence peak, showing that the state in Eq. (3) can be detected by this setup. On the other hand, for the state in Eq. (4), there is a coincidence dip at the same delay. It is also due to the quantum interference in the 50:50 fiber coupler, which make the two photons output from the same ports of the coupler. The visibility of the curves corresponding coincidence peak and dip are 83%. It can be expected that similar results can be expected if another two Bell states are tested by this setup. Hence, it is demonstrated that by the proposed scheme, the polarization entangled Bell states can be generated successfully, and the pairs in the state of Eq. (3) can be discriminated by the simplified polarization BSM setup.

In the experiment, the optical filters for the pump lights and signal/idler photons have the same bandwidths, hence, although the generated photons are frequency-degenerate, the indistinguishability of them is limited. It impacts the measured visibility of the coincidence peak and dip [26]. It can be expected that higher visibility, i.e., better discrimination ability of the Bell states generated by this scheme, could be realized if narrower filter bandwidth of signal/idler photons is used to improve the indistinguishability. It also can be expected that all the four polarization entangled Bell states could be prepared on the generated photon pairs by

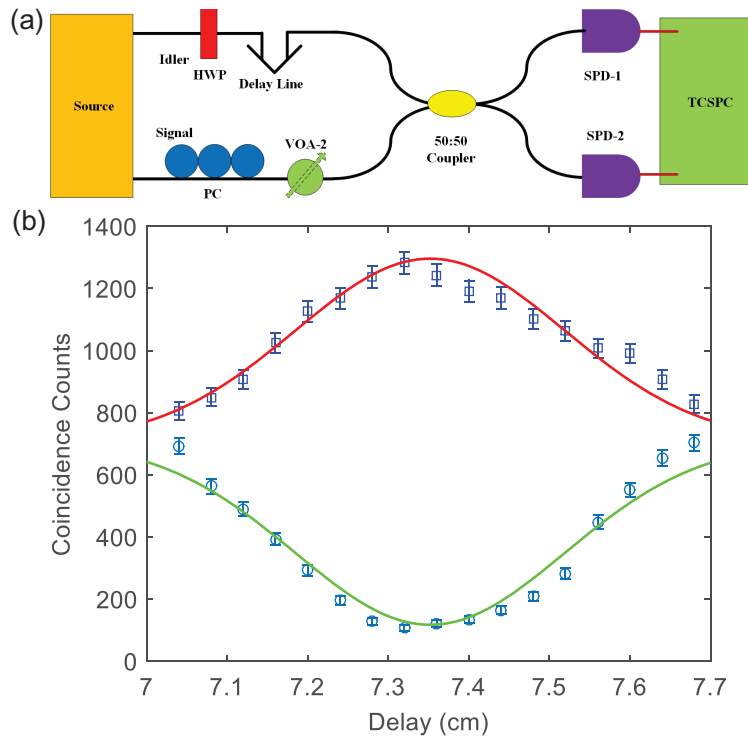


Fig. 5. The experiment of BSM on the generated polarization-entangled Bell states. (a) the setup. VOA: variable optical attenuator. PC: polarization controller. SPD: single photon detector. TCSPC: time correlated single photon counting module. (b) The coincidence number of two states under different optical delay. The hollow squares and circles show the curves corresponding the states in Eq. (3) and Eq. (4), respectively. The visibility of the curve is 83%

proper polarization manipulation, which can be fully discriminated if improved BSM scheme is applied on them.

4. Conclusion

In this paper, we proposed a generation scheme of telecom band frequency-degenerate polarization entangled photon pairs based on optical fibers. It utilizes the vector SFWM process in a Sagnac fiber loop, by which frequency-degenerate and polarization orthogonal biphoton states are generated along the CW and CCW directions, respectively. The quantum interference between them at the 50:50 fiber coupler of the fiber loop separates the two photons, leading to the generation of polarization entanglement. This scheme is demonstrated experimentally, the raw fringe visibilities of the two-photon interferences under two non-orthogonal polarization bases are 91% and 90%. Due to the property of frequency-degenerate, polarization entangled Bell states can be prepared on the generated photon pairs, which can be discriminated by the BSM. It is demonstrated by a simplified BSM setup, which can discriminate the anti-symmetric polarization entangled Bell state. The visibility of the coincidence peak and dip of the BSM experiment is 83%, showing that the proposed scheme can be used to generate polarization entangled Bell pairs, which can be used to carry information by their property of quantum entanglement.

Funding

973 Programs of China (2013CB328700 and 2011CBA00303); National Natural Science Foundation of China (61575102 and 61321004); Tsinghua University Initiative Scientific Research Program (20131089382).